Analysis of the October 3–7 2000 GEM storm with the WINDMI model

W. Horton and E. Spencer
Institute for Fusion Studies, University of Texas, Austin, Texas, USA

I. Doxas
Center for Integrated Plasma Studies, University of Colorado, Boulder, Colorado, USA

J. Kozyra
Department of Atmospheric, Oceanic and Space Sciences, University of Michigan, Ann Arbor, Michigan, USA

Received 18 May 2005; revised 12 September 2005; accepted 10 October 2005; published 17 November 2005.

[1] The 8 dimensional physics model WINDMI is used to analyze the October 3–7, 2000 geomagnetic storm using solar wind input data from the ACE satellite. This period was chosen because it contains an extended interval of well-defined and quasi-periodic auroral activations called sawtooth oscillations, a phenomena whose relationship to substorm processes and to upstream solar wind drivers is still under debate. The question of whether multiple sawtooth oscillations are triggered by periodic upstream solar wind features or by internal magnetospheric processes is addressed. The model predicts both the occurrence of 8 auroral activations identified as sawtooth events during the 24 hour period on the 4th of October, in agreement with the measured AL index, and also an earlier multiple sawtooth interval on the 3rd of October, in agreement with the measured AL index. These intervals occur during steady but moderate solar wind IMF Bz values and the periodicity of the sawtooth events was not directly related to any periodic features in the upstream solar wind. The model also predicts the geomagnetic Dst index through the main and recovery phase of the storm.
Citation: Horton, W., E. Spencer, I. Doxas, and J. Kozyra (2005), Analysis of the October 3–7 2000 GEM storm with the WINDMI model, *Geophys. Res. Lett.*, *32*, L22102, doi:10.1029/2005GL023515.

1. Introduction

[2] It is becoming increasingly evident that the solar wind (WIND) driven magnetosphere-ionosphere (MI) is a complex dynamical system. The challenge associated with modeling and prediction of the state of this system has been described as ''the space weather problem'' by researchers. The magnetosphere formed by the solar wind plasma interacting with the almost dipolar magnetic field of the earth contains numerous energy reservoirs and transitional layers that separate the nightside geomagnetic lobes, central plasma sheet, and inner-magnetospheric ring current. The solar wind electric field drives substantial power through these components, a large fraction of which is dissipated in the ionosphere and ring current through charge exchange collisions with neutral atoms. The character of such a complex weather system is that it may exhibit a variety of bifurcations and limited long time predictability from finitely accurate initial conditions.

[3] The WINDMI model, an eight dimensional model of the solar wind driven magnetosphere-ionosphere system, was developed to explore the complexity of this system. It is widely recognized that auroral zone disturbances that result from responses of this system take on a variety of forms. Classifications now include: 1) poleward boundary intensifications, 2) periodic substorms, 3) sawtooth events, 4) isolated substorms, and 5) dynamic pressure-driven activations [*Lyons*, 2000; *Henderson*, 2004]. *Horton et al.* [2003] have used the WINDMI model to classify three types of substorms based on 1) a bimodal response with an internal trigger based on the near-Earth neutral line model, 2) a rapid unloading initiated by a northward turning of the IMF, and 3) a linear filter response. With this framework, the WINDMI model successfully reproduced three types of substorms [*Horton et al.*, 2003] in a database with 117 isolated substorms [*Blanchard and McPherron*, 1993]. Here we use the present version of WINDMI [*Doxas et al.*, 2004; *Horton et al.*, 2005] to explore the 3–7 October 2000 magnetospheric response to moderate and slowly varying inputs from a magnetic cloud that swept past the Earth over more than a 40-hour period, producing several intervals of quasi-periodic auroral activity.

[4] The model proceeds by decomposing the magnetosphere-ionosphere system into the magnetotail lobe, the central plasma sheet, the region 1 and region 2 currents and the ring current. The power flow of the relevant partial differential equations are then projected onto key global energy variables. The physical dimensions of the regions do not change with time, which is a limitation of the model. The two largest energy components are (1) the magnetic energy W_m stored in the geotail lobes that extend to a distance L_x behind the Earth and (2) the plasma energy $W_{\rm rc}$ in the ring current.

[5] The depression of the terrestrial mid-latitude surface magnetic field measured by the $D_{\rm st}$ index is calculated from $W_{\rm rc}$ using the Dessler-Parker-Schopke relation [*Kivelson and Russell*, 1995]. The field aligned current I_1 (R1 FAC) closes the divergence ($\nabla \cdot \mathbf{j} = 0$) of the electric current $\mathbf{j}$ in the nightside magnetosphere through the nightside auroral ionosphere and is the principal component of the lower

0094-8276/05/2005GL023515$05.00

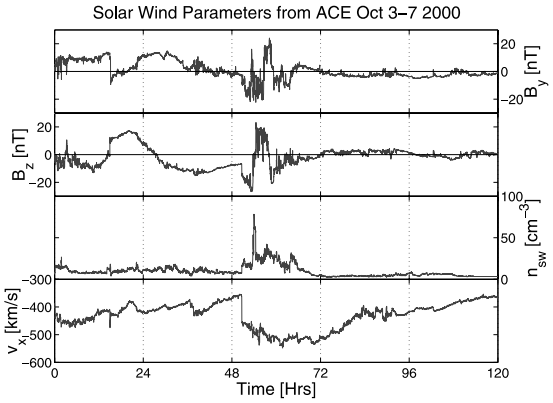

Figure 1. ACE satellite measurement of the solar wind velocity v_x, proton density n_p, IMF B_z and B_y components for 3–7 October 2000. The satellite was located at approximately $X = 224$, $Y = -29$, $Z = -5$ Earth radii in GSM coordinates during this period. See color version of this figure in the HTML.

auroral (AL) geomagnetic index used to define substorms. This current has an associated magnetic energy $\frac{1}{2}L_1 I_1^2$ where L_1 is the self-inductance of the loop. The loop also contains magnetic flux Φ_{MI} through a mutual inductance M with the larger ($\sim$20 times) geotail cross-field current loop $I(t)$. Both current loops have associated voltages V, V_I driven by the solar wind dynamo voltage $V_{sw}(t)$. The resultant electric fields give rise to $\mathbf{E} \times \mathbf{B}$ perpendicular plasma flows whose energies are stored in the capacitances C and C_I. The high pressure plasma trapped by the reversed lobe magnetic fields gives the thermal energy component $U_p = \frac{3}{2}p\Omega_{cps}$, where $\Omega_{cps} = L_x L_y L_z$ is the volume of the central plasma sheet. The parallel kinetic energy $K_{\|}$ is due to plasma flow along magnetic field lines.

2. Storm Data

[6] In Figure 1 we show the ACE satellite solar wind and IMF data for October 3–7 2000. An extended magnetic cloud began at 10:18 UT on October 3 and continued until 05:34 UT on October 5 [*Wang et al.*, 2003]. A high speed solar wind stream following the magnetic cloud compressed and enhanced the southward IMF in the trailing edge of the cloud, greatly increasing its geoeffectiveness and leading to a major magnetic storm that lasted from October 3–7 but only reached its most disturbed levels shortly after the trailing edge of the magnetic cloud passed the Earth. The solar wind data correlates with measurements of the westward auroral AL index and the D_{st} index on the same dates. The AL index and D_{st} index (shown in Figures 2 and 3) are from the World Data Center at Kyoto University.

[7] Of interest in the present storm, two separate intervals of periodic substorm activity occur: one from about 08:00–16:00 UT on October 3 and the other from about 06:00–22:00 UT on October 4. The activity in the later interval has been identified as sawtooth oscillations by *Huang et al.* [2003]. The earlier interval has comparable characteristics but was not discussed in that reference. Sawtooth events have many similarities to large periodic substorms but extend over a broader than usual range of local times and penetrate anomalously close to Earth for long intervals [*Henderson*, 2004]. They are driven during storms by moderate ($B_z < -10$nT) but slowly varying southward IMF. There is debate whether these are periodic substorms or a different form of geomagnetic activity. There is also debate whether this activity is triggered by features in the solar wind or results from internal magnetospheric processes. WINDMI can contribute to this debate by analyzing its ability to predict both the timing within the storm interval and periodicity of the sawtooth events.

[8] In Figure 2 we show the energetic electron and proton flux data as measured by the LANL satellite 1989–046 to highlight the substorm injection events that occur on October 4 2000. We observe that the AL index has a sawtooth auroral waveform for every injection event measured by the LANL satellite.

3. WINDMI Analysis

3.1. Model Description

[9] The dynamo voltage V_{sw} is calculated in two ways. The first is to use the rectified voltage $V_{sw} = v_{sw} B_s^{IMF} L_y^{eff}$ where v_{sw} is the x-directed component of the solar wind velocity in GSM coordinates, B_s^{IMF} is the southward IMF component and L_y^{eff} is an effective cross-tail width over which the dynamo voltage is produced. The second method uses a formula given by *Siscoe et al.* [2002] and *Ober et al.* [2003] for the coupling of the solar wind to the magnetopause using solar wind dynamic pressure P_{sw} to determine the stand-off distance. This formula is given by,

$$V_{sw}(kV) = 30.0(kV) + 57.6 E_{sw}(mV/m) P_{sw}^{-1/6}(nPa) \qquad (1)$$

where $E_{sw} = v_{sw}(B_y^2 + B_z^2)^{1/2}\sin(\frac{\theta}{2})$ is the solar wind electric field and $P_{sw} = n_{sw} m_p v_{sw}^2$. Here m_p is the mass of a proton. The IMF clock angle θ is taken to be $\tan^{-1}(B_y/B_z)$. The solar wind flow velocity v_{sw} is assumed to be v_x while n_{sw} is the solar wind proton density. Additionally, V_{sw} is delayed to account for solar wind propagation from the ACE satellite to the nose of the bow shock using the formula in *Bargatze et al.* [1985].

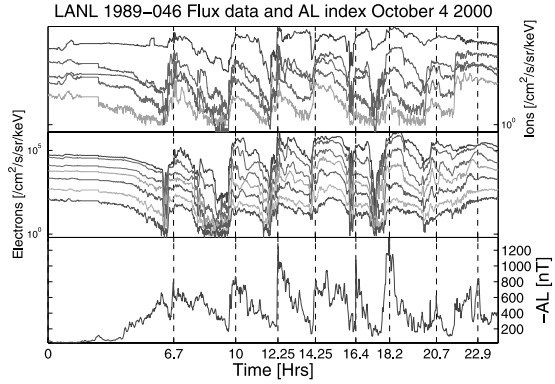

Figure 2. October 4 2000 energetic proton and electron flux injection measurements from the LANL 1989–046 spectrometers, lined up with the measured geomagnetic AL index showing the 8 substorm peaks correlated to the injection events. See color version of this figure in the HTML.

[10] The state vector $X = (I, V, p, K_{\|}, I_1, V_I, I_2, W_{\rm rc})$ in the WINDMI model is given by the equations:

$$L\frac{dI}{dt} = V_{\rm sw}(t) - V + M\frac{dI_1}{dt} \tag{2}$$

$$C\frac{dV}{dt} = I - I_1 - I_{\rm ps} - \Sigma V \tag{3}$$

$$\frac{3}{2}\frac{dp}{dt} = \frac{\Sigma V^2}{\Omega_{\rm cps}} - u_0 p K_{\|}^{1/2}\Theta(u) - \frac{pVA_{\rm eff}}{\Omega_{\rm cps}B_{\rm tr}L_y} - \frac{3p}{2\tau_{\rm E}} \tag{4}$$

$$\frac{dK_{\|}}{dt} = I_{ps}V - \frac{K_{\|}}{\tau_{\|}} \tag{5}$$

$$L_1\frac{dI_1}{dt} = V - V_I + M\frac{dI}{dt} \tag{6}$$

$$C_I\frac{dV_I}{dt} = I_1 - I_2 - \Sigma_I V_I \tag{7}$$

$$L_2\frac{dI_2}{dt} = V_I - \left(R_{\rm prc} + R_{\rm A2}\right)I_2 \tag{8}$$

$$\frac{dW_{\rm rc}}{dt} = R_{\rm prc}I_2^2 + \frac{pVA_{\rm eff}}{B_{\rm tr}L_y} - \frac{W_{\rm rc}}{\tau_{\rm rc}} \tag{9}$$

The quantities L, C, Σ, L_1, C_I and Σ_I are the magnetospheric and ionospheric inductances, capacitances, and conductances respectively. A_{eff} is an effective aperture for particle injection into the ring current. The resistances in the partial ring current and region-2 current I_2 regions are $R_{\rm prc}$ and $R_{\rm A2}$ respectively, and L_2 is the inductance of the region-2 current. u_0 is a heat flux limiting parameter. The confinement times for the central plasma sheet, parallel kinetic energy and ring current are τ_E, $\tau_{\|}$ and $\tau_{\rm rc}$. The effective width of the magnetosphere is L_y and the transition region magnetic field is given by $B_{\rm tr}$. The pressure gradient driven current is given by $I_{ps} = L_x(p/\mu_0)^{1/2}$ where L_x is the effective length of the magnetotail. The pressure unloading function $\Theta(u) = \frac{1}{2}[1 + \tanh u]$ where $u = (I - I_c)/\Delta I$ in Equation (4) is specified by a critical current I_c and the interval ΔI for the transition to loss of plasma along newly opened magnetic field lines with a parallel thermal flux $q_{\|}$. The unloading function follows from current gradient driven tearing modes or cross-field current instabilities, as described by *Yoon et al.* [2002]. The parameters are combined into a vector $\mathbf{P}^{\rm d}$ where $d = 18$.

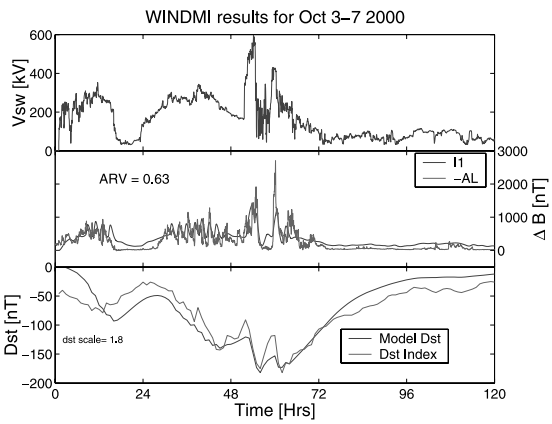

Figure 3. WINDMI output I_1 and scaled Dst compared to the measured indices using manually optimized parameters. Here the Siscoe derived solar wind dynamo of equation (1) is used. See color version of this figure in the HTML.

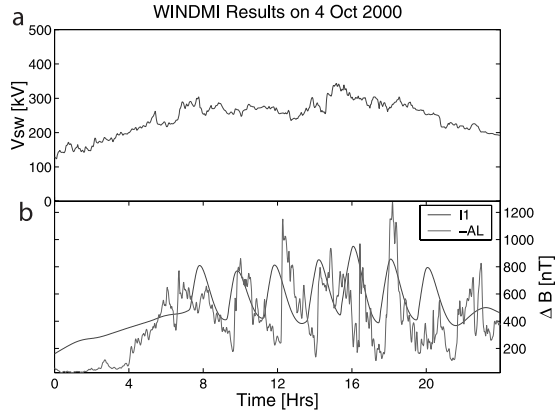

Figure 4. Details of the *AL* prediction from a manually tuned WINDMI model with the AL data for October 4 2000. (a) Top panel is the solar wind dynamic pressure modulated input dynamo voltage from equation (1). (b) The output signal AL (I_1) from equations (2)–(9) against the AL data. See color version of this figure in the HTML.

3.2. Results

[11] Using nominal parameters from physics estimates and the rectified input voltage, the predicted AL has average relative variance ARV = 0.78 when compared to the AL index. Changing to the Siscoe solar wind voltage improves the comparison slightly, to ARV = 0.74. The average relative variance obtained when the parameters were tuned manually improved considerably to ARV = 0.63 while still using the Siscoe input. The ARV improves to 0.58 when we used a genetic algorithm (GA) to find the optimal parameter vector $\mathbf{P}$ with respect to the AL data, but the GA solution does not display the periodic substorms. Here we manually selected a parameter set to obtain a solution that has low ARV with respect to the AL index and captures the eight substorms that occur in the main phase of the storm. The parameters that strongly influence the oscillations are the capacitance C of the central plasma sheet, the level of the critical current I_c and the parallel heat flux limit parameter u_0 (see auxiliary material[1]).

[12] Figure 3 compares the predicted $D_{\rm st}$ and measured $D_{\rm st}$ for the nominal parameter vector. The agreement in the shape of the waveform is good. For both the AL and $D_{\rm st}$ signals the network system does not capture the high frequency components. This deficiency is serious in the two very sharp peaks of large AL data at 07:00 UT and 12:00 UT shown in Figure 3 on October 5 at the end of the

[1]Auxiliary material is available at ftp://ftp.agu.org/apend/gl/2005GL023515.

main phase of the storm. The model gives a peak AL of about 1200 nT for both peaks at roughly the correct time but the AL index has narrower peaks going up to 1500 nT at 07:00 UT and to 3000 nT at 12:00 UT on 5 October.

[13] On Oct 4 2000 eight peaks of AL data ranging from 600nT to 1300 nT appear on average every 2 hours. These are the sawtooth oscillations that are seen as particle injections by the LANL geosynchronous spacecraft. The correspondence between the AL and LANL satellite data during these injection events is shown in Figure 2. That the model captures these events, as shown in Figure 4, is important since the injections produce the 300keV seed electrons in the inner magnetosphere, some fraction of which are eventually accelerated to become the multi-MeV (killer) electrons of *Summers et al.* [1998] and *Baker et al.* [1998].

[14] While the framework for explanation of the quasi periodic episodes of substorm injections is the same as given by *Huang and Reeves* [2005], the present model differs in detail from their qualitative picture. The WINDMI model requires sufficient energy build-up in the central plasma sheet during the main phase of the storm in order to trigger a series of unloading events. The intrinsic global Alfven eigenmodes of the geotail with periods as long as one to two hours, appealed to by *Huang and Reeves* [2005], are contained in the WINDMI model but are not sufficient to predict the substorms. This null conclusion has been tested through variations of the model without the unloading physics and appears to be provable by a detailed stability analysis of strongly driven steady states in the absence of an unloading mechanism.

4. Conclusions

[15] A plasma physics based network model called WINDMI is used to calculate eight energy components in the solar wind driven magnetosphere-ionosphere-ring current system. The parameters of the system are estimated a priori within physically realizable ranges. The 3–7 October 2000 storm is then examined in detail, using results obtained with manually tuned parameters. Key features and conclusions are that:

[16] 1. The internal trigger for unloading plasma pressure allows the model to show the substorm and sawtooth oscillations, with the timing and relative amplitudes in rough agreement with the AL index and the LANL energetic particle data. External solar wind triggers are not required.

[17] 2. During two intervals within the magnetic cloud when the IMF is <-10nT and slowly varying, WINDMI predicts periodic substorm activity in which the timing and duration closely reproduces the AL signature. This is in agreement with the observations that moderate but steady solar wind driving produces sawtooth events [*Henderson*, 2004].

[18] 3. Eight substorms occur on October 4 with associated sawtooth injections of electrons (50–750 keV) and protons (75–670 keV) recorded by the LANL geosynchronous spacecraft. The model qualitatively captures these eight injection events, thus it may be coupled to dipolarization pulse models [*Li et al.*, 1998; *Baker et al.*, 1998] to yield estimates for the electron flux trapped in the inner magnetosphere. These electron fluxes are the seed populations for the MeV-energy electron radiation belts formed approximately one day after the storm recovery.

[19] 4. The system satisfies charge and energy conservation, and thus may have an advantage over ARMA and neural networks when the database is too small to train data-driven prediction filters.

[20] **Acknowledgments.** This work was partially supported by NSF grant ATM-0229863. J. Kozyra would like to acknowledge support for this work under NASA grant NNG05GJ89G and NSF grant ATM-0402163. The authors also wish to acknowledge Los Alamos National Labs for the LANL 1989-046 satellite data.

References

Baker, D., X. Li, J. Blake, and S. Kanekal (1998), Strong electron acceleration in the Earth's magnetosphere, *Adv. Space Res.*, *21*(4), 609.

Bargatze, L. F., D. N. Baker, R. L. McPherron, and E. W. Hones Jr. (1985), Magnetospheric impulse response for many levels of geomagnetic activity, *J. Geophys. Res.*, *90*(A7), 6387.

Blanchard, G., and R. McPherron (1993), A bimodal representation of the response function relating the solar wind electric field to the AL index, *Adv. Space Res.*, *13*(4), 71.

Doxas, I., W. Horton, W. Lin, S. Seibert, and M. Mithaiwala (2004), A dynamical model for the coupled inner magnetosphere and tail, *IEEE Trans. Plasma Sci.*, *32*(4), 1443.

Henderson, M. (2004), May 2–3, 1986 CDAW-9C interval: A sawtooth event, *Geophys. Res. Lett.*, *31*, L11804, doi:10.1029/2004GL019941.

Horton, W., R. S. Weigel, D. Vassiliadis, and I. Doxas (2003), Substorm classification with the WINDMI model, *Nonlinear Processes Geophys.*, *10*, 363.

Horton, W., M. Mithaiwala, E. Spencer, and I. Doxas (2005), WINDMI: A family of physics network models for storms and substorms, in *Multi-Scale Coupling of Sun-Earth Processes*, edited by A. Lui, Y. Kamide, and G. Consolini, Elsevier, New York.

Huang, C., and G. Reeves (2005), Periodic substorms: A new periodicity of 2–3 hours in the magnetosphere, in *Multi-Scale Coupling of Sun-Earth Processes*, edited by A. Lui, Y. Kamide, and G. Consolini, Elsevier, New York.

Huang, C.-S., G. Reeves, J. Borovsky, R. Skoug, Z. Pu, and G. Le (2003), Periodic magnetospheric substorms and their relationship with solar wind variations, *J. Geophys. Res.*, *108*(A6), 1255, doi:10.1029/2002JA009704.

Kivelson, M., and C. Russell (Eds.) (1995), *Introduction to Space Physics*, Cambridge Univ. Press, New York.

Li, X., D. Baker, M. Temerin, G. Reeves, and R. Belian (1998), Simulation of dispersionless injections and drift echoes of energetic electrons associated with substorms, *Geophys. Res. Lett.*, *25*(20), 3763.

Lyons, L. (2000), Geomagnetic disturbances: Characteristics of, distinction between types, and relations to interplanetary conditions, *J. Atmos. Sol. Terr. Phys.*, *62*, 1087.

Ober, D. M., N. C. Maynard, and W. J. Burke (2003), Testing the Hill model of transpolar potential saturation, *J. Geophys. Res.*, *108*(A12), 1467, doi:10.1029/2003JA010154.

Siscoe, G. L., G. M. Erickson, B. U. O. Sonnerup, N. C. Maynard, J. A. Schoendorf, K. D. Siebert, D. R. Weimer, W. W. White, and G. R. Wilson (2002), Hill model of transpolar potential saturation: Comparisons with MHD simulations, *J. Geophys. Res.*, *107*(A6), 1075, doi:10.1029/2001JA000109.

Summers, D., R. Thorne, and F. Xiao (1998), Relativistic theory of wave-particle resonant diffusion with application to electron acceleration in the magnetosphere, *J. Geophys. Res.*, *103*(A9), 20,487.

Wang, Y., P. Ye, S. Wang, and X. Xue (2003), An interplanetary cause of large geomagnetic storms: Fast forward shock overtaking preceding magnetic cloud, *Geophys. Res. Lett.*, *30*(13), 1700, doi:10.1029/2002GL016861.

Yoon, P., A. Lui, and M. Sitnov (2002), Generalized lower-hybrid drift instabilities in current sheet equilibrium, *Phys. Plasmas*, *9*(5), 1526.

I. Doxas, Center for Integrated Plasma Studies, University of Colorado, Boulder, CO 80309-0390, USA.

W. Horton and E. Spencer, Institute for Fusion Studies, RLM 11.222, University of Texas, Austin, TX 78712-0262, USA. (horton@physics.utexas.edu)

J. Kozyra, Department of Atmospheric, Oceanic and Space Sciences, University of Michigan, Ann Arbor, MI 48109-2143, USA.